

Supporting Information

Effects of Residual Disinfectant on the Redox Speciation of Lead (II)/(IV)

Minerals in Drinking Water Distribution Systems

Sumant Avasarala^a, John Orta^a, Michael Schaefer^b,

Macon Abernathy^b, Samantha Ying^b, and Haizhou Liu^{a*}

^a Department of Chemical and Environmental Engineering, University of California, Riverside,
Riverside, CA 92521 USA

^b Department of Environmental Sciences, University of California, Riverside, Riverside, CA
92521 USA

*Corresponding author, e-mail: haizhou@engr.ucr.edu,

phone (951) 827-2076, fax (951) 827-5696

Table of Contents

I. Text.....	S5
Text S1: Chemical equilibrium modeling using the Geochemist’s Work Bench software.....	S5
Text S2: Modelling second-order solid-phase reaction kinetics of Pb(II) mineral oxidation.....	S7
Text S3: Modeling drinking water distribution systems using representative concentrations.	S9
IV. Tables.....	S10
Table S1: Relevant reduction and oxidation equations with real reduction potential under different chemical conditions.....	S10
III. Figures.....	S11
Figure S1: Equilibrium diagram showing the effect of higher chloride concentration [Cl ⁻] on lead speciation, in drinking water systems utilizing phosphate addition as a lead control strategy. Bolded line represents the total dissolved Pb(II) concentration. Red dashed line represents the USEPA MCL for lead. T = 20°C, ionic strength = 0.01M, TOTCO ₃ = 1 mM, [Cl ⁻] = 1 mM, [PO ₄ ³⁻] = 0.5 mg/L.	S11
Figure S2: Estimation of reaction rate constant ($k^{\text{HOCl}}_{\text{Cerussite}}$) for cerussite (Cer) oxidation using HOCl, where C^{Cer}_t , C^{Cer}_0 and C^{HOCl}_t , C^{HOCl}_0 refer to concentrations of cerussite and HOCl at time time = t and time = 0, respectively.....	S12
Figure S3: Linear combination fitting of lead carbonate EXAFS spectra during oxidation by HOCl. a) Cerussite c) Hydrocerussite. Percentage distribution of Pb(II) and Pb(IV) minerals in the solids during lead phosphate oxidation by HOCl. Linear combination fitting (represented by dashed lines) of the EXAFS spectra, b) Cerussite d) Hydrocerussite.....	S13
Figure S4: XRD spectra of lead solids during cerussite oxidation by free chlorine. TOTCO ₃ = 10 mM, [HOCl] ₀ = 4.2 g/L as Cl ₂ , initial Cl ₂ :Pb(II)=3:1, T=22°C, pH=7.....	S14
Figure S5: Estimation of reaction rate constant ($k^{\text{HOCl}}_{\text{Hydrocerussite}}$) for hydrocerussite (Hcer) oxidation using HOCl, where C^{Hcer}_t , C^{Hcer}_0 and C^{HOCl}_t , C^{HOCl}_0 refer to concentrations of hydrocerussite and HOCl at time time = t and time = 0, respectively.....	S15

Figure S6: Chloropyromorphite oxidation by HOCl. $\text{TOTCO}_3 = 10 \text{ mM}$, $[\text{HOBr}]_0 = 4.2 \text{ g as Cl}_2/\text{L}$, initial $\text{HOCl:Pb(II)}=3:1$, $T=22^\circ\text{C}$, $\text{pH}=7$ **(a)** XANES of CPM oxidation; $[\text{Pb}_5(\text{PO}_4)_3\text{Cl}_{(s)}]_0 = 5 \text{ g/L}$ **(b)** Lead speciation in CPM oxidation. S16

Figure S7: Hydroxylpyromorphite oxidation by HOCl. $\text{TOTCO}_3 = 10 \text{ mM}$, $[\text{HOBr}]_0 = 4.2 \text{ g as Cl}_2/\text{L}$, initial $\text{HOCl:Pb(II)}=3:1$, $T=22^\circ\text{C}$, $\text{pH}=7$ **(a)** XANES of hydroxylpyromorphite oxidation; $[\text{Pb}_5(\text{PO}_4)_3\text{OH}_{(s)}]_0 = 5 \text{ g/L}$ **(b)** Lead speciation in hydroxylpyromorphite oxidation.....S17

Figure S8: XRD spectra of lead solids during oxidation by free chlorine. $\text{TOTCO}_3 = 10 \text{ mM}$, $[\text{HOCl}]_0 = 4.2 \text{ g/L as Cl}_2$, initial $\text{Cl}_2:\text{Pb(II)}=3:1$, $T=22^\circ\text{C}$, $\text{pH}=7$. **a)** Hydroxylpyromorphite **b)** PyromorphiteS18

Figure S9: Estimation of reaction rate constant ($k^{\text{HOBr}}_{\text{Cerussite}}$) for cerussite oxidation using HOBr, where C^{Cer}_t , C^{Cer}_0 and C^{HOBr}_t , C^{HOBr}_0 refer to concentrations of cerussite and HOBr at time t and time $= 0$, respectively.....S19

Figure S10: Estimation of reaction rate constant ($k^{\text{HOBr}}_{\text{Hydrocerussite}}$) for hydrocerussite oxidation using HOBr, where C^{Hcer}_t , C^{Hcer}_0 and C^{HOBr}_t , C^{HOBr}_0 refer to concentrations of hydrocerussite and HOBr at time t and time $= 0$, respectively.....S20

Figure S11: XRD spectra of lead solids during cerussite oxidation by free bromine. $\text{TOTCO}_3 = 10 \text{ mM}$, $[\text{HOBr}]_0 = 4.2 \text{ g/L as Cl}_2$, initial $\text{Cl}_2:\text{Pb(II)}=3:1$, $T=22^\circ\text{C}$, $\text{pH}=7$S21

Figure S12: Linear combination fitting of lead carbonate EXAFS spectra during oxidation by HOBr. **a)** Cerussite **c)** Hydrocerussite. Percentage distribution of Pb(II) and Pb(IV) minerals in the solids during lead phosphate oxidation by HOBr. Linear combination fitting of the EXAFS spectra, **b)** Cerussite **d)** Hydrocerussite..... S22

Figure S13: Estimation of reaction rate constant ($k^{\text{HOBr}}_{\text{Hydroxylpyromorphite}}$) for hydroxylpyromorphite (HPM) oxidation using HOBr, where C^{HPM}_t , C^{HPM}_0 and C^{HOBr}_t , C^{HOBr}_0 refer to concentrations of hydroxylpyromorphite and HOBr at time t and time $= 0$, respectively.....S23

Figure S14: Estimation of reaction rate constant ($k^{\text{HOBr}}_{\text{Chloropyromorphite}}$) for chloropyromorphite (CPM) oxidation using HOBr, where C^{CPM}_t , C^{CPM}_0 and C^{HOBr}_t , C^{HOBr}_0 refer to concentrations of chloropyromorphite and HOBr at time t and time $= 0$, respectively.....S24

Figure S15: EXAFS spectra of lead phosphate oxidation by HOBr **a)** Hydroxypyromorphite **c)** Chloropyromorphite. Percentage distribution of Pb(II) and Pb(IV) minerals in the solids during lead phosphate oxidation by HOBr. Linear combination fitting (represented by dashed lines) of the EXAFS spectra, **b)** Hydroxypyromorphite **d)** Chloropyromorphite.....S25

Figure S16: XRD spectra of lead solids during pyromorphite oxidation by free bromine. $\text{TOTCO}_3 = 10 \text{ mM}$, $[\text{HOBr}]_0 = 4.2 \text{ g/L}$ as Cl_2 , initial $\text{Cl}_2:\text{Pb(II)}=3:1$, $T=22^\circ\text{C}$, $\text{pH}=7$S26

Figure S17: Dissolved oxygen (DO) measurement during lead phosphates oxidation by HOBr. $\text{TOTCO}_3 = 10 \text{ mM}$, $[\text{HOBr}]_0 = 4.2 \text{ g/L}$ (59.2 mM) as Cl_2 , initial $[\text{HOBr}]:[\text{Pb(II)}]=3:1$, $T=22^\circ\text{C}$, $\text{pH}=7$. **(a)** hydroxypyromorphite oxidation; **(b)** chloropyromorphite oxidation.....S27

Text S1: Chemical equilibrium modeling using the Geochemist's Work Bench software

Equilibrium constants of reactions involving lead(II) species were obtained from the Visual MINTEQ database, except the solubility product (K_{sp}) of phosphohedyphane $Pb_3Ca_2(PO_4)_3Cl_{(s)}$ that was experimentally obtained and added to the software database. Solubility experiments with $Pb_3Ca_2(PO_4)_3Cl_{(s)}$ were conducted to calculate its K_{sp} value. Specifically, a 1g/L suspension of phosphohedyphane was brought to an equilibrium condition at pH 7 with an ionic strength of 10 mM using $NaClO_4$. The solution was continuously stirred, and samples were drawn then filtered through a 0.22- μ m filter. Samples were then analyzed via inductively coupled plasma - mass spectroscopy (ICP-MS) and ion chromatograph (IC) to quantify the concentrations of lead [Pb^{+2}], calcium [Ca^{2+}] and chloride [Cl^-], respectively. The following equation was used to calculate K_{sp} of phosphohedyphane, 1.0×10^{-76} where, γ_{Pb} , γ_{Ca} and γ_{Cl} were the activity coefficients of lead, calcium and chloride. Considering the low ionic strength and assuming ideal behavior, these activity coefficients were approximated to 1.

$$K_{sp} = (\gamma_{Pb}[Pb^{2+}])^3 * (\gamma_{Ca})^2 * (\gamma_{Cl})$$

Drinking water chemical parameters including pH, alkalinity, chloride, calcium and phosphate concentrations were varied to predict their effects on the predominance of Pb(II) minerals. Alkalinity (TOTCO₃) and hardness were varied between 5 and 100 mg/L as CaCO₃. Similarly, phosphate level ranged between 0 and 2 mg/L as PO₄³⁻, corresponding to no orthophosphate treatment and the upper limit of corrosion control dosage. Chloride addition was varied from 3.5-250 mg/L, simulating from a low-chloride condition to the secondary chloride MCL set by

the U.S. EPA. Using this updated database, geochemical modelling was conducted to identify the formation of different Pb(II) minerals under relevant drinking water conditions.

Text S2: Modelling second-order solid-phase reaction kinetics of Pb(II) mineral oxidation

Reaction kinetics of solid-phase transformation of Pb(II) minerals to Pb(IV) by an oxidant (*i.e.*, either chlorine or bromine) was modelled based on the consumption rate of Pb(II) solid reactants as below:

$$\frac{d[Pb(II)]}{dt} = -k_{Pb(II)} [Pb(II)_{(s)}] [Ox] S_{Pb(II)(s)} \quad (\text{Equation 1})$$

Where, $k_{Pb(II)}$ is the rate constant for Pb(II) mineral oxidation reaction in $L \cdot m^{-2} \cdot min^{-1}$, $[Pb(II)_{(s)}]$ is the concentration of Pb(II) in the solids in g/L, $[Ox]$ is the oxidant (HOCl/HOBr) concentration in g of Cl_2/L and $S_{Pb(II)(s)}$ is the specific surface area in m^2/g of the Pb(II) mineral undergoing the oxidation reaction. The specific surface area of the Pb(II) solids used in this manuscript were measured to be 1.18, 5.45, 16.84 and 1.63 m^2/g for cerussite, hydrocerussite, hydroxyl pyromorphite and chloropyromorphite, respectively.

Prior to the reaction, the reactant concentrations, $[Pb(II)_{(s)}]$ and $[Ox]$, are 5g/L and $\sim 4.2g Cl_2/L$; however, these concentrations change, as the product $[PbO_2]$ is formed. Therefore, at a time t when a known concentration 'X' of the product is formed, then the reactant concentrations change to $[Pb(II)_{(s)} - X]$ and $[Ox - X]$. Using this information, equation 1 can now be rewritten as:

$$\frac{d[Pb(II)]}{dt} = -k_{Pb(II)} [Pb(II)_{(s)} - X] [Ox - X] S_{Pb(II)(s)} \quad (\text{Equation 2})$$

Rearranging components and integrating equation 2:

$$\int_0^X \frac{d[Pb(II)]}{[Pb(II)_{(s)} - X] [Ox - X]} = -k_{Pb(II)} S_{Pb(II)(s)} \int_0^t dt \quad (\text{Equation 3})$$

Since solving this equation cannot be directly integrated, the method of partial fractions was introduced, and the following relationship for reaction rate constant k was developed:

$$k = \frac{1}{t} * \frac{1}{SSA} * \frac{1}{[Pb(II)_{(s)}]_0 - [Ox]_0} \ln \left(\frac{[Pb(II)_{(s)}]_t * [Ox]_0}{[Pb(II)_{(s)}]_0 * [Ox]_t} \right) \quad (\text{Equation 4})$$

$[Pb(II)_{(s)}]_0$ and $[Ox]_0$, and $[Pb(II)_{(s)}]_t$ and $[Ox]_t$ represent the initial concentration and the concentration at time t of solids and oxidant in the system. This rate constant (k) was then optimized using a model to predict Pb(II) concentrations and compared to the experimental results. Fitting parameters were solved to reach a targeted R^2 of 1 ± 0.05 , a slope of 1 ± 0.1 and an intercept of 0 ± 0.05 .

Text S3: Modeling drinking water distribution systems using representative concentrations.

Drinking water distribution systems were modeled using kinetic coefficients derived from experimental data as described in text S2. Typical drinking water conditions that include an Ionic strength (IS) = 1mM, [HOCl] = $7.04 \cdot 10^{-6}$ M/L (0.5mg/L), pH = 7, T = 22°C, were used for the model. The bromide concentrations were varied between $0-4.05 \cdot 10^{-5}$ M/L (0-3.2mg/L); therefore, any bromide present in the drinking water was assumed to react instantaneously with free chlorine, forming free bromine. Both bromide and chlorine concentrations in the drinking water distribution systems were assumed to be in steady state, with a 90% oxidative transformation of Pb(II) to Pb(IV) as the targeted time frame. The equation was written as follows:

$$\frac{dPb(II)}{dt} = -k_{HOCl}C_{Pb(II)}C_{HOCl} - k_{HOBr}C_{Pb(II)}C_{HOBr} \quad (\text{Equation 5})$$

Where k_{HOCl} ($L \cdot m^{-2} \cdot min^{-1}$) is the *second* order rate constant for each Pb(II) mineral with free chlorine, k_{HOBr} ($L \cdot m^{-2} \cdot min^{-1}$) is the *second* order rate constant for each Pb(II) mineral with free bromine, $C_{Pb(II)}$ is the concentration of Pb(II) minerals, C_{HOCl} (M/L) is the concentration of free chlorine, and C_{HOBr} (M/L) is the concentration of free bromine. Integration and solving of the equation yield the following equation:

$$\ln \left(\frac{C_{Pb(II)t}}{C_{Pb(II)0}} \right) = -(k_{HOCl}C_{HOCl} + k_{HOBr}C_{HOBr})\Delta t \quad (\text{Equation 6})$$

Where $C_{Pb(II)0}$ is the initial concentration of Pb(II), $C_{Pb(II)t}$ is the concentration at time t , and Δt is the elapsed time. Assuming 90% conversion, $\ln\left(\frac{C_{Pb(II)t}}{C_{Pb(II)0}}\right)$ can be substituted with $\ln(0.1)$ and the equation solved for Δt to get total time for oxidation of Pb(II) solids.

Table S1 Relevant reduction and oxidation equations with real reduction potential under different chemical conditions.

No.	Redox Reactions	Standard E (V)	Actual E (V)*	Experimental E (V)**
1	$\text{HOCl}_{(\text{aq})} + \text{H}^+ + 2e^- \rightleftharpoons \text{Cl}^- + \text{H}_2\text{O}$	1.482	1.22	1.26
2	$\beta\text{-PbO}_{2(\text{s})} + \text{CO}_3^{2-} + 4\text{H}^+ + 2e^- \rightleftharpoons \text{PbCO}_{3(\text{s})} + 2\text{H}_2\text{O}$	1.46	0.55	0.58
3	$3\beta\text{-PbO}_{2(\text{s})} + 2\text{CO}_3^{2-} + 10\text{H}^+ + 6e^- \rightleftharpoons \text{Pb}_3(\text{CO}_3)_2(\text{OH})_{2(\text{s})} + 4\text{H}_2\text{O}$	1.46	0.71	0.74
4	$\text{HOBr}_{(\text{aq})} + \text{H}^+ + 2e^- \rightleftharpoons \text{Br}^- + \text{H}_2\text{O}$	1.34	1.13	1.13
5	$5\beta\text{-PbO}_{2(\text{s})} + 20\text{H}^+ + 10e^- + 3\text{PO}_4^{3-} + \text{Cl}^- \rightleftharpoons \text{Pb}_5(\text{PO}_4)_3\text{Cl}_{(\text{s})} + 10\text{H}_2\text{O}$	1.46	0.52	0.60
6	$5\beta\text{-PbO}_{2(\text{s})} + 19\text{H}^+ + 10e^- + 3\text{PO}_4^{3-} \rightleftharpoons \text{Pb}_5(\text{PO}_4)_3\text{OH}_{(\text{s})} + 9\text{H}_2\text{O}$	1.46	0.57	0.64
7	$\text{O}_2 + 2\text{H}_2\text{O} + 4e^- \rightleftharpoons 4\text{OH}^-$	0.40	0.81	0.81

* Typical drinking water condition: ionic strength = 10 mM, $[\text{Cl}^-] = 1 \text{ mM}$, $[\text{HOCl}] = 8.7 \text{ }\mu\text{M}$, $[\text{PO}_4^{3-}] = 5.3 \text{ }\mu\text{M}$, $\text{TOTCO}_3 = 1 \text{ mM}$, $\text{pH} = 7$. $[\text{HOBr}] = 1 \text{ }\mu\text{M}$, $[\text{Br}^-] = 1 \text{ }\mu\text{M}$.

** Experimental condition used in this study: $[\text{HOCl}] = 59.2 \text{ mM}$, $\text{TOTCO}_3 = 10 \text{ mM}$, $[\text{PO}_4^{3-}] = 5.8 \text{ mM}$, $[\text{Cl}^-] = 39.4 \text{ mM}$, $\text{pH} = 7$, $[\text{HOBr}] = 59.2 \text{ mM}$, $[\text{Br}^-] = 65.12 \text{ mM}$.

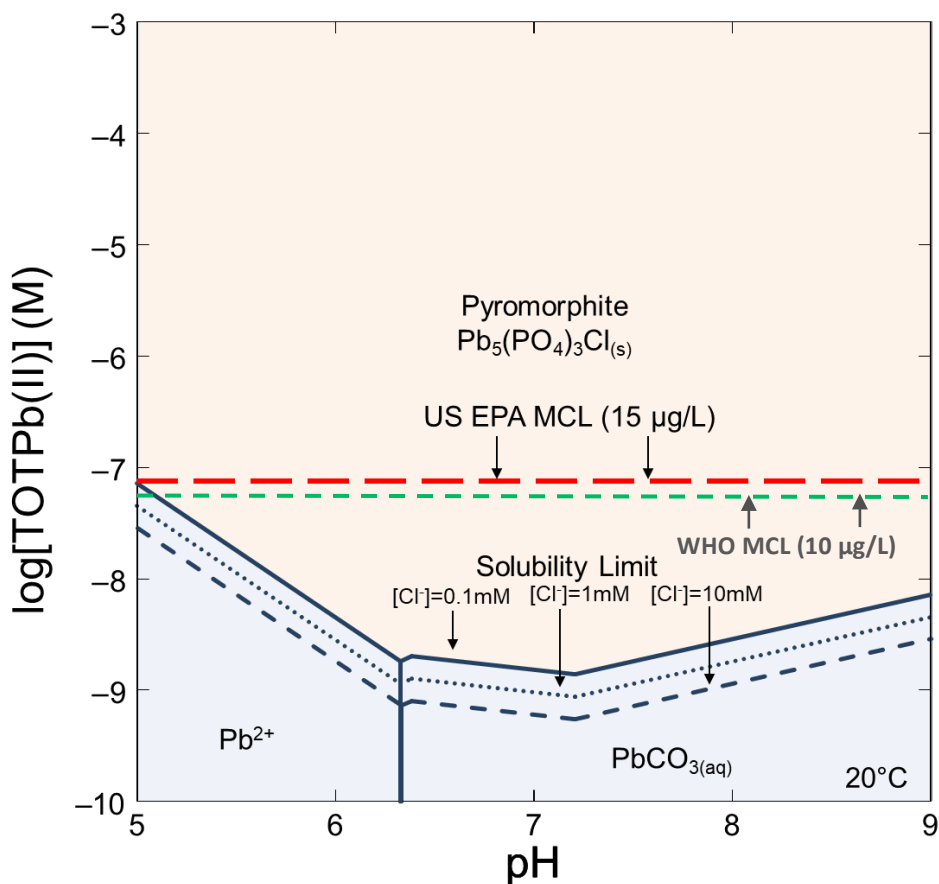


Figure S1 Equilibrium diagram showing the effect of higher chloride concentration $[Cl^-]$ on lead speciation, in drinking water systems utilizing phosphate addition as a lead control strategy. Bolded line represents the total dissolved Pb(II) concentration. Red and the green dashed line represent the USEPA and WHO MCL for lead. $T = 20^\circ C$, ionic strength = 0.01M, $TOTCO_3 = 1$ mM, $[Cl^-] = 1$ mM, $[PO_4^{3-}] = 0.5$ mg/L.

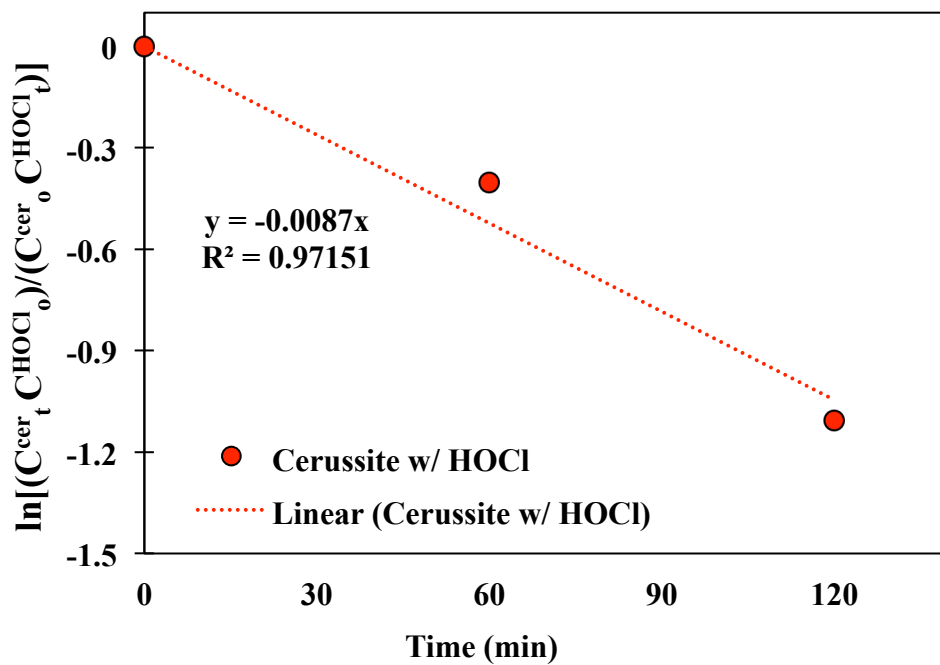


Figure S2 Estimation of reaction rate constant ($k^{\text{HOCl}}_{\text{Cerussite}}$) for cerussite (Cer) oxidation using HOCl, where C^{Cer}_t , C^{Cer}_0 and C^{HOCl}_t , C^{HOCl}_0 refer to concentrations of cerussite and HOCl at time time = t and time = 0, respectively.

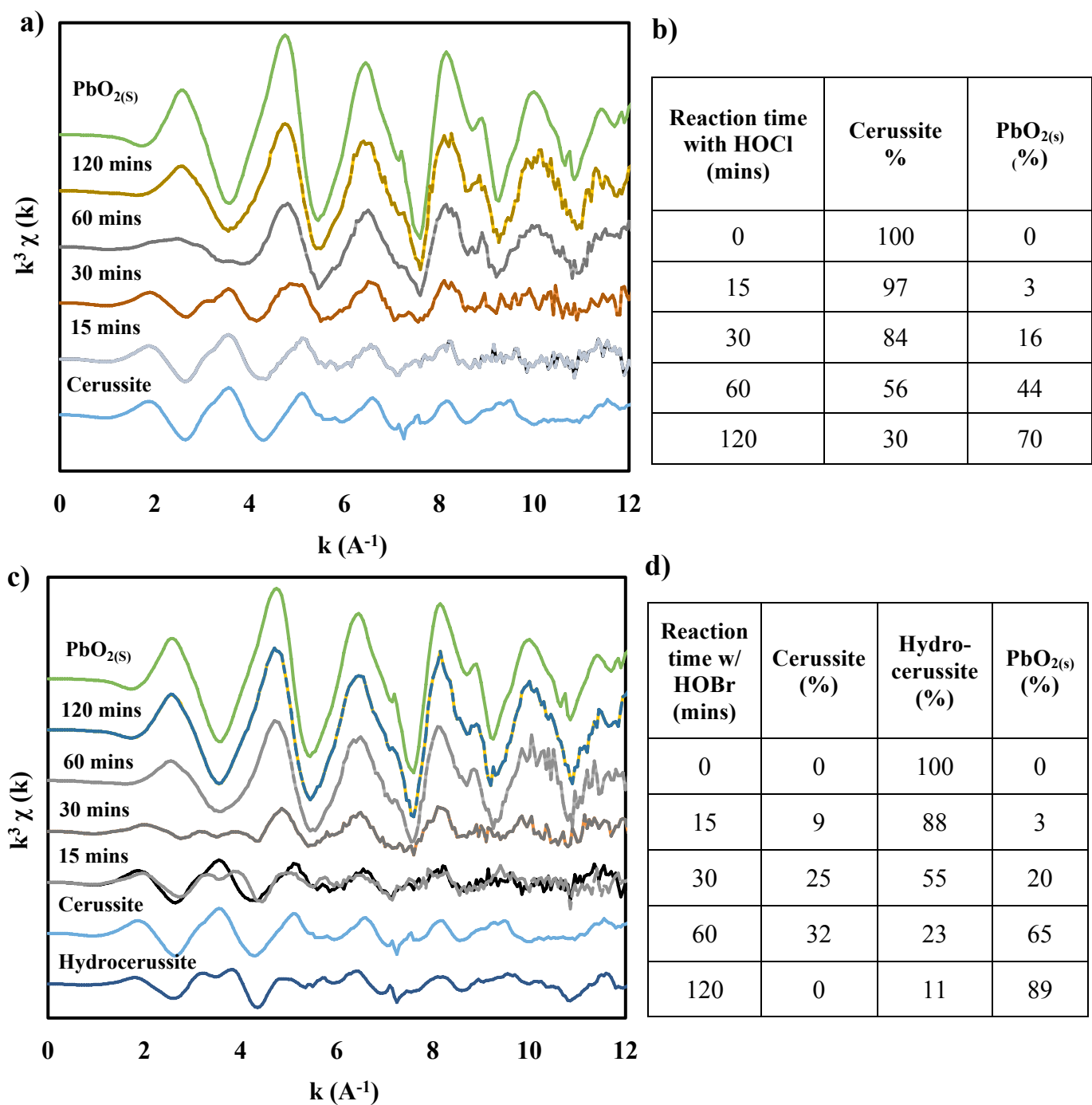


Figure S3 Linear combination fitting of lead carbonate EXAFS spectra during oxidation by HOCl. **a)** Cerussite **c)** Hydrocerussite. Percentage distribution of Pb(II) and Pb(IV) minerals in the solids during lead phosphate oxidation by HOCl. Linear combination fitting (represented by dashed lines) of the EXAFS spectra, **b)** Cerussite **d)** Hydrocerussite.

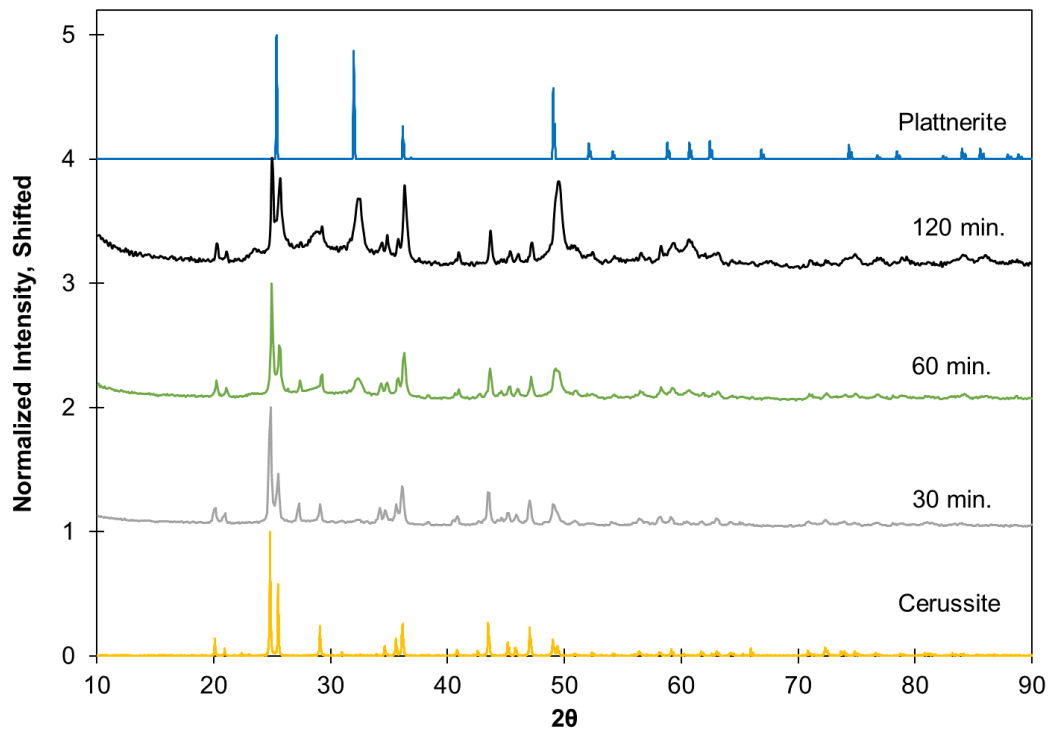


Figure S4 XRD spectra of lead solids during cerussite oxidation by free chlorine. $\text{TOTCO}_3 = 10$ mM, $[\text{HOCl}]_0 = 4.2$ g/L as Cl_2 , initial $\text{Cl}_2:\text{Pb(II)}=3:1$, $T=22^\circ\text{C}$, $\text{pH}=7$.

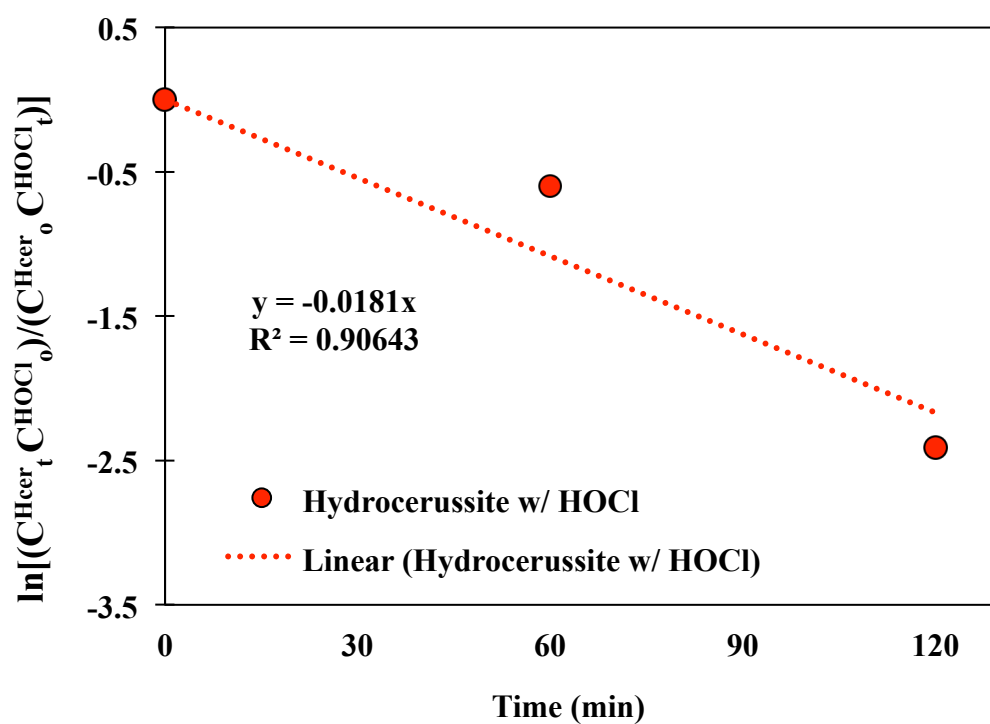


Figure S5: Estimation of reaction rate constant ($k^{\text{HOCl}}_{\text{Hydrocerussite}}$) for hydrocerussite (Hcer) oxidation using HOCl, where C^{Hcer}_t , C^{Hcer}_0 and C^{HOCl}_t , C^{HOCl}_0 refer to concentrations of hydrocerussite and HOCl at time t and time 0 , respectively.

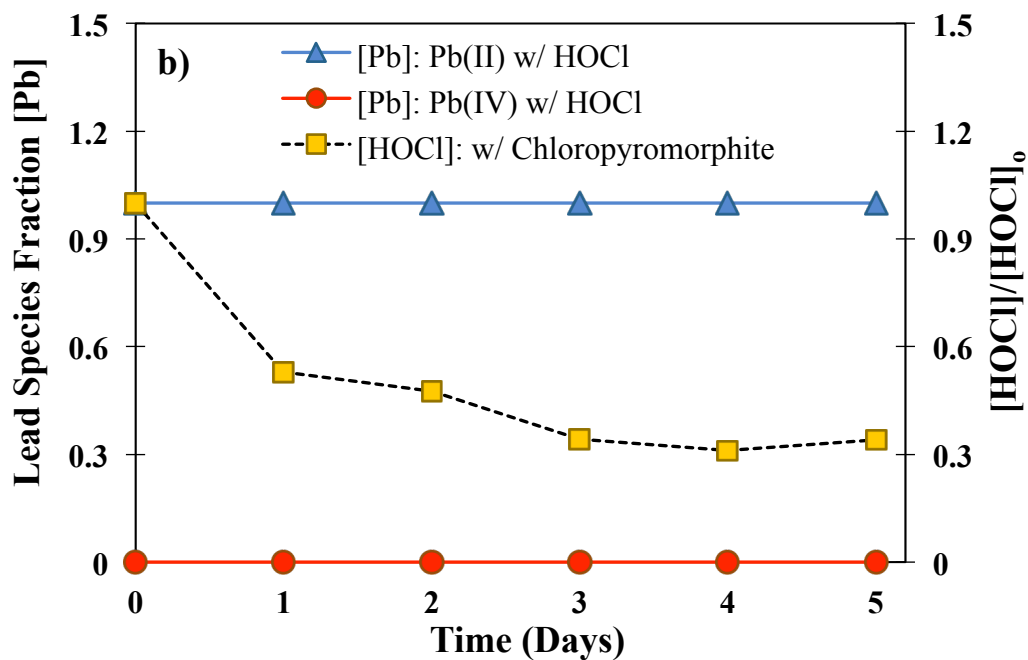
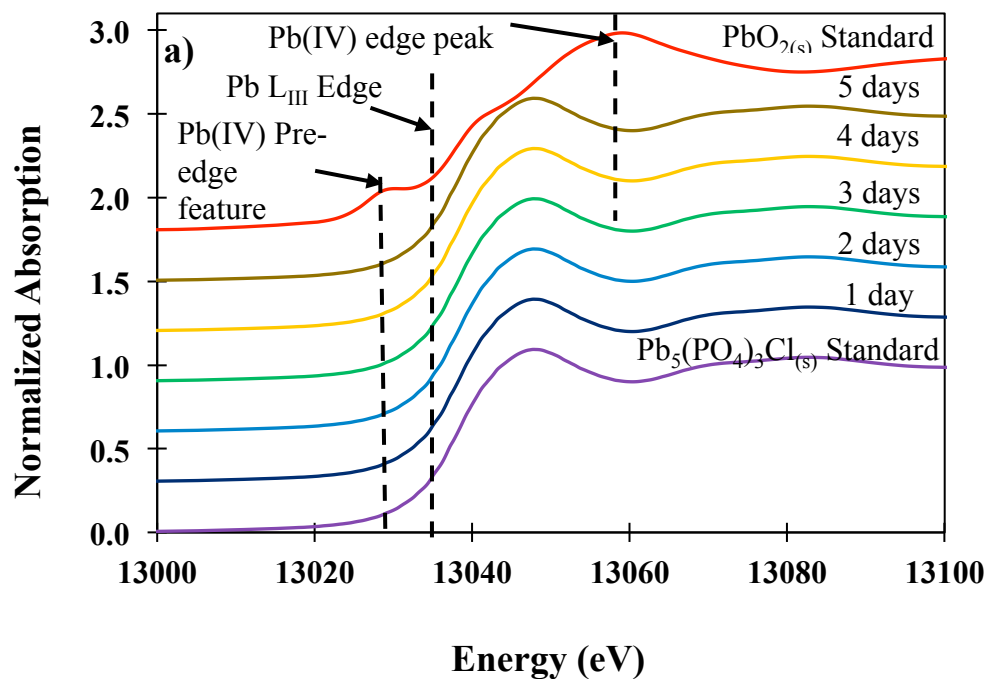


Figure S6 Chloropyromorphite oxidation by HOCl. $\text{TOTCO}_3 = 10 \text{ mM}$, $[\text{HOBr}]_0 = 4.2 \text{ g as Cl}_2/\text{L}$, initial $\text{HOCl}:\text{Pb(II)}=3:1$, $T=22^\circ\text{C}$, $\text{pH}=7$ **(a)** XANES of CPM oxidation; $[\text{Pb}_5(\text{PO}_4)_3\text{Cl}_{(s)}]_0 = 5 \text{ g/L}$ **(b)** Lead speciation in CPM oxidation.

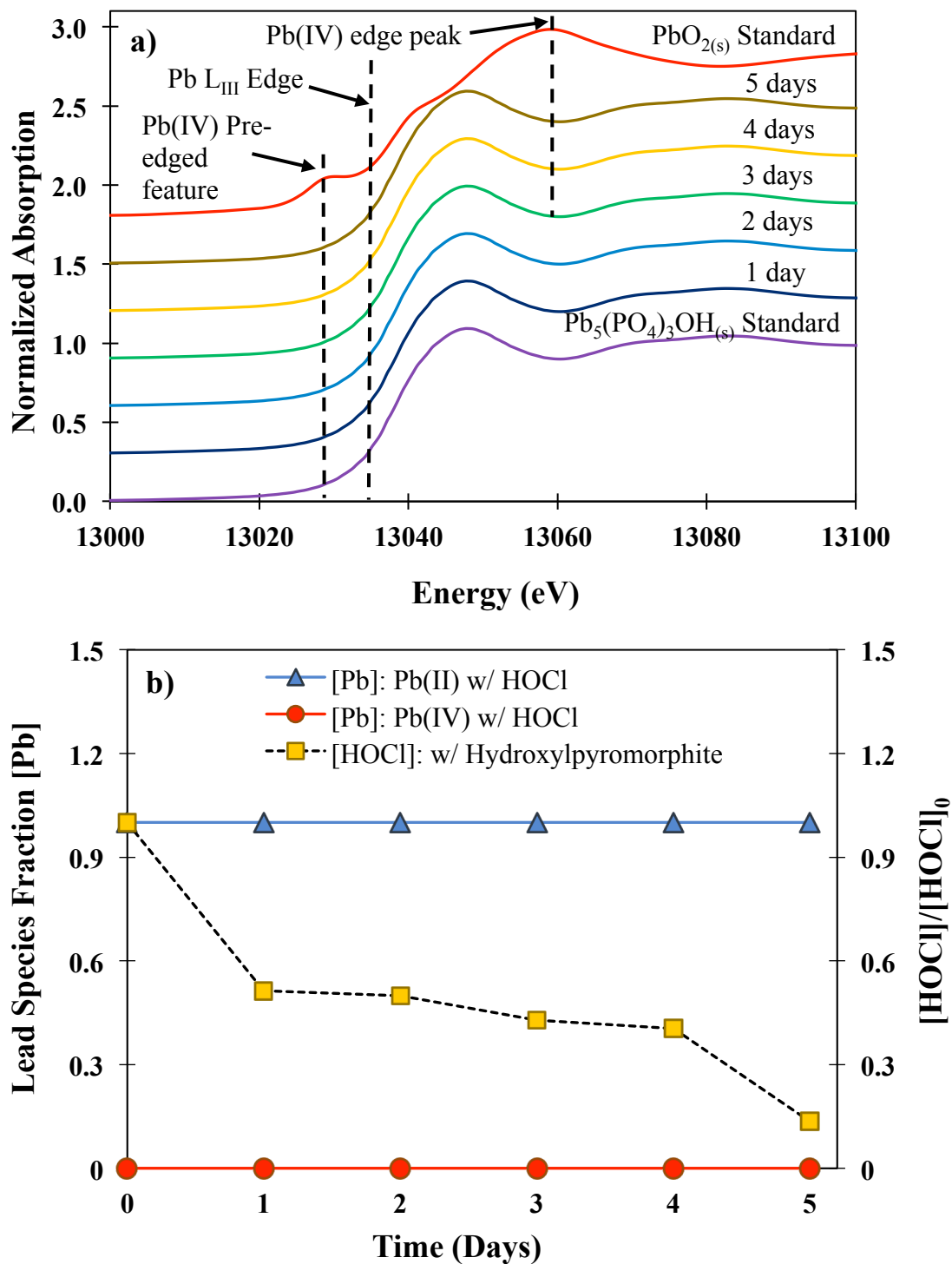


Figure S7 Hydroxylpyromorphite oxidation by HOCl. TOTCO₃ = 10 mM, [HOBr]₀ = 4.2 g as Cl₂/L, initial HOCl:Pb(II)=3:1, T=22°C, pH=7 **(a)** XANES of hydroxylpyromorphite oxidation; [Pb₅(PO₄)₃OH_(s)]₀ = 5 g/L **(b)** Lead speciation in hydroxylpyromorphite oxidation.

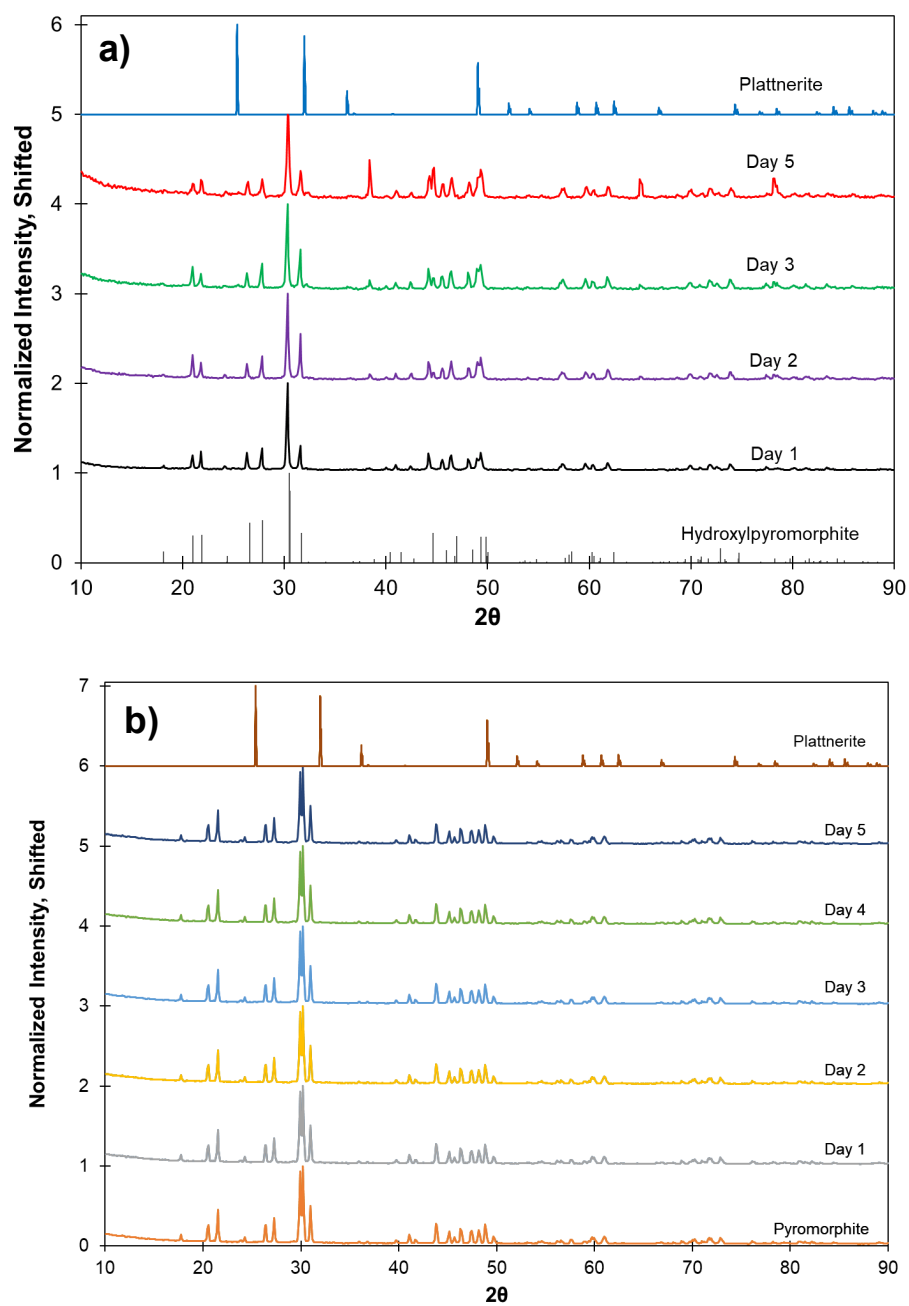


Figure S8 XRD spectra of lead solids during oxidation by free chlorine. $\text{TOTCO}_3 = 10 \text{ mM}$, $[\text{HOCl}]_0 = 4.2 \text{ g/L}$ as Cl_2 , initial $\text{Cl}_2:\text{Pb(II)}=3:1$, $T=22^\circ\text{C}$, $\text{pH}=7$. **a)** Hydroxypyromorphite **b)** Pyromorphite

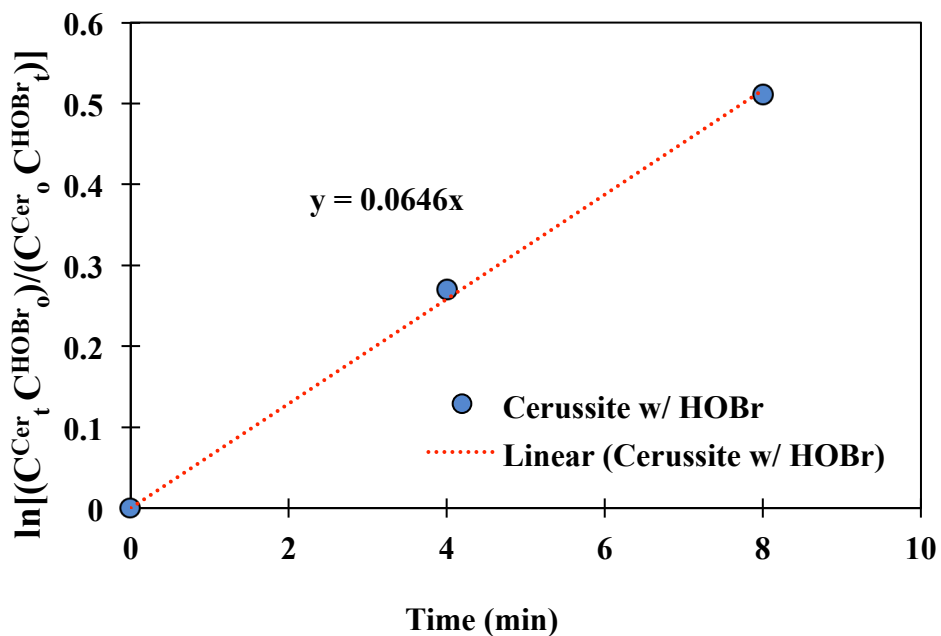


Figure S9 Estimation of reaction rate constant ($k^{\text{HOBr}}_{\text{Cerussite}}$) for cerussite oxidation using HOBr, where C^{Cer}_t , C^{Cer}_0 and C^{HOBr}_t , C^{HOBr}_0 refer to concentrations of cerussite and HOBr at time t and time $= 0$, respectively.

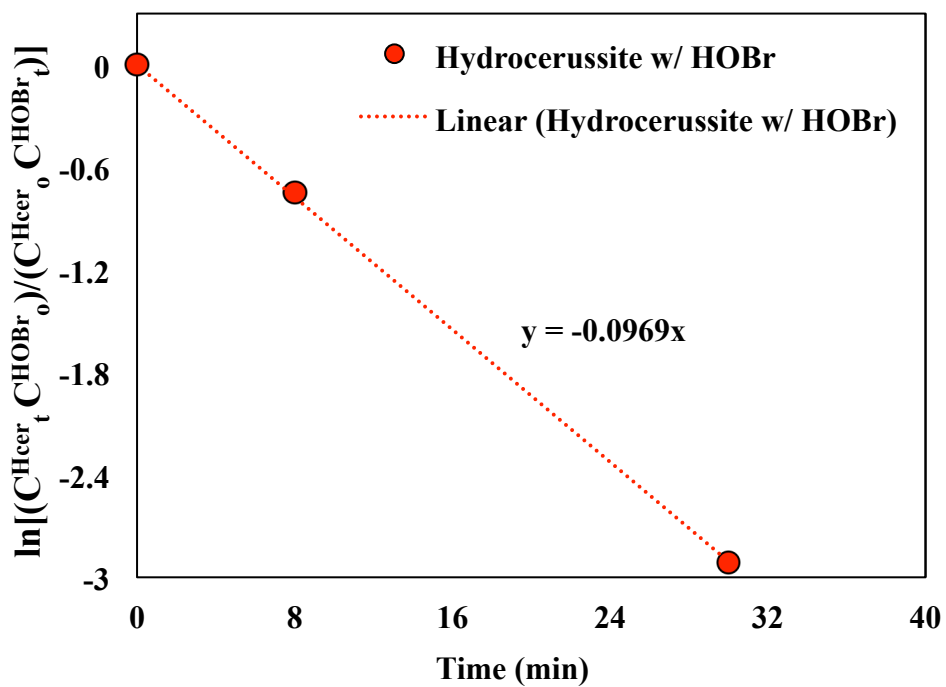


Figure S10 Estimation of reaction rate constant ($k^{\text{HOBr}}_{\text{Hydrocerussite}}$) for hydrocerussite oxidation using HOBr, where C^{Hcer}_t , C^{Hcer}_0 and C^{HOBr}_t , C^{HOBr}_0 refer to concentrations of hydrocerussite and HOBr at time t and time $= 0$, respectively.

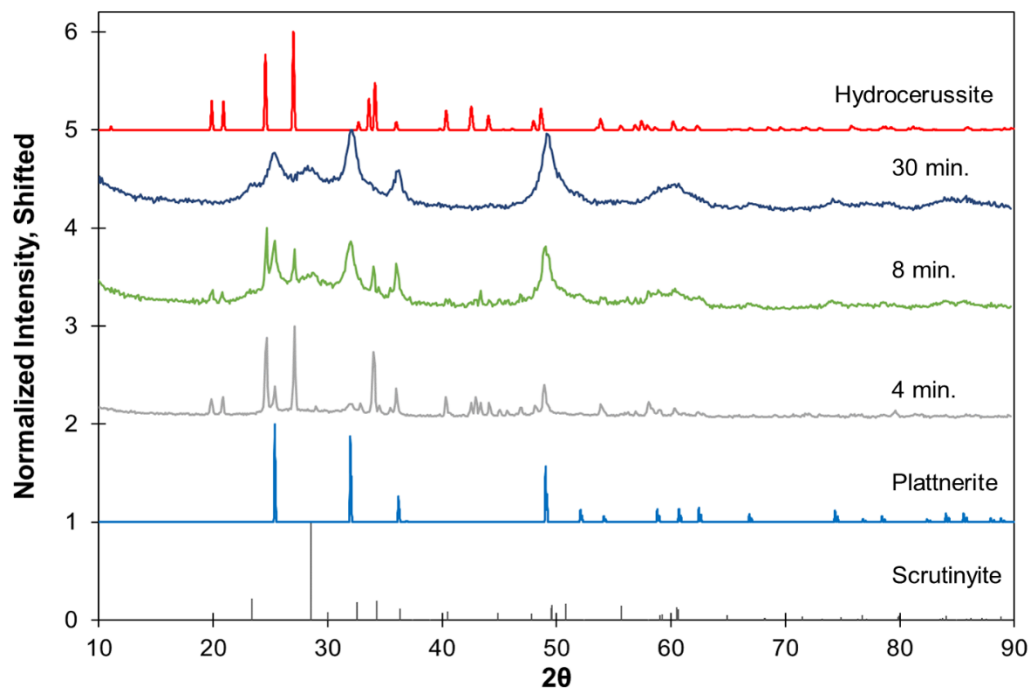


Figure S11 XRD spectra of lead solids during cerussite oxidation by free bromine. $\text{TOTCO}_3 = 10 \text{ mM}$, $[\text{HOBr}]_0 = 4.2 \text{ g/L as Cl}_2$, initial $\text{Cl}_2:\text{Pb(II)}=3:1$, $T=22^\circ\text{C}$, $\text{pH}=7$.

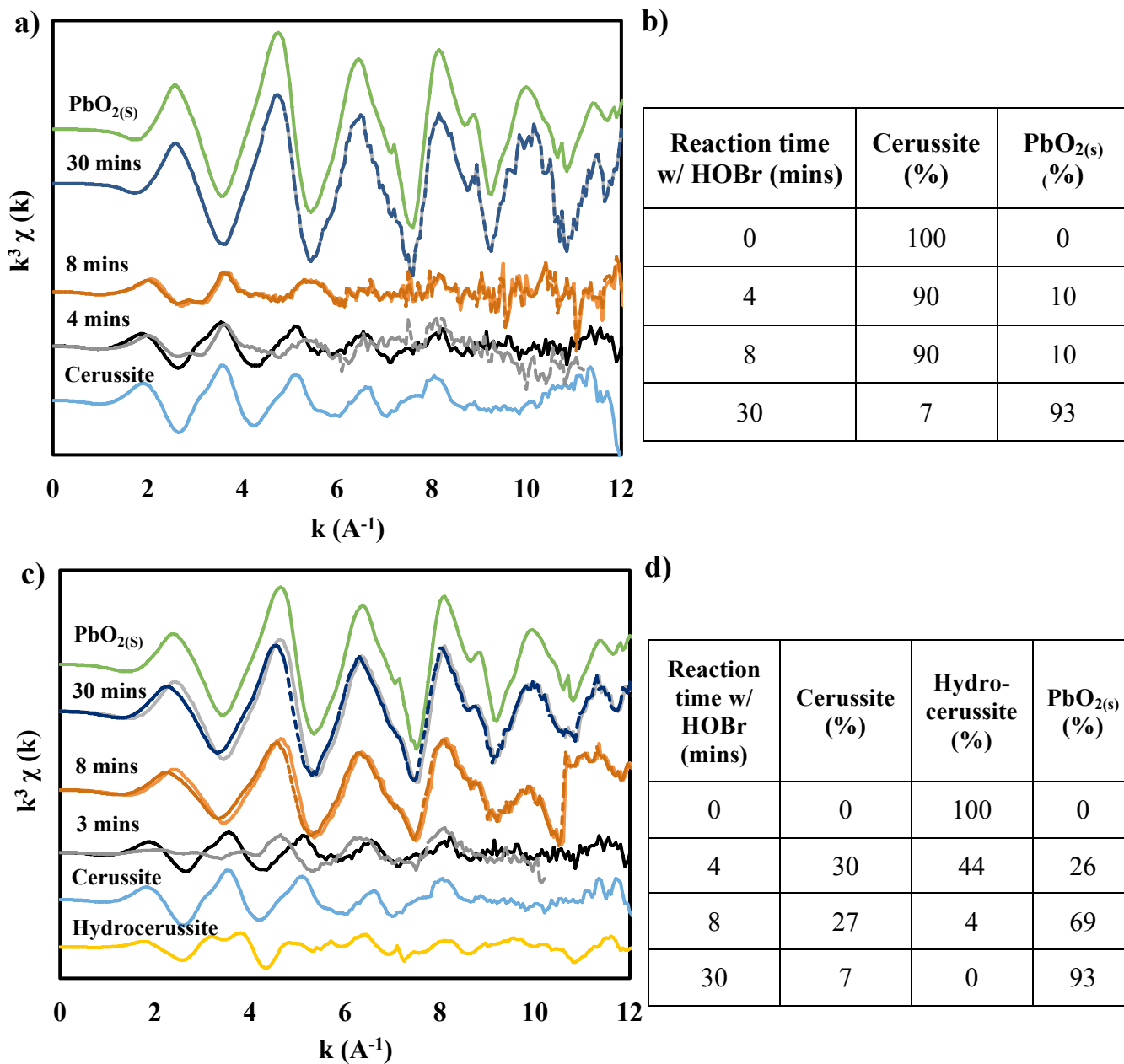


Figure S12 Linear combination fitting of lead carbonate EXAFS spectra during oxidation by HOBr. **a)** Cerussite **c)** Hydrocerussite. Percentage distribution of Pb(II) and Pb(IV) minerals in the solids during lead phosphate oxidation by HOBr. Linear combination fitting of the EXAFS spectra, **b)** Cerussite **d)** Hydrocerussite.

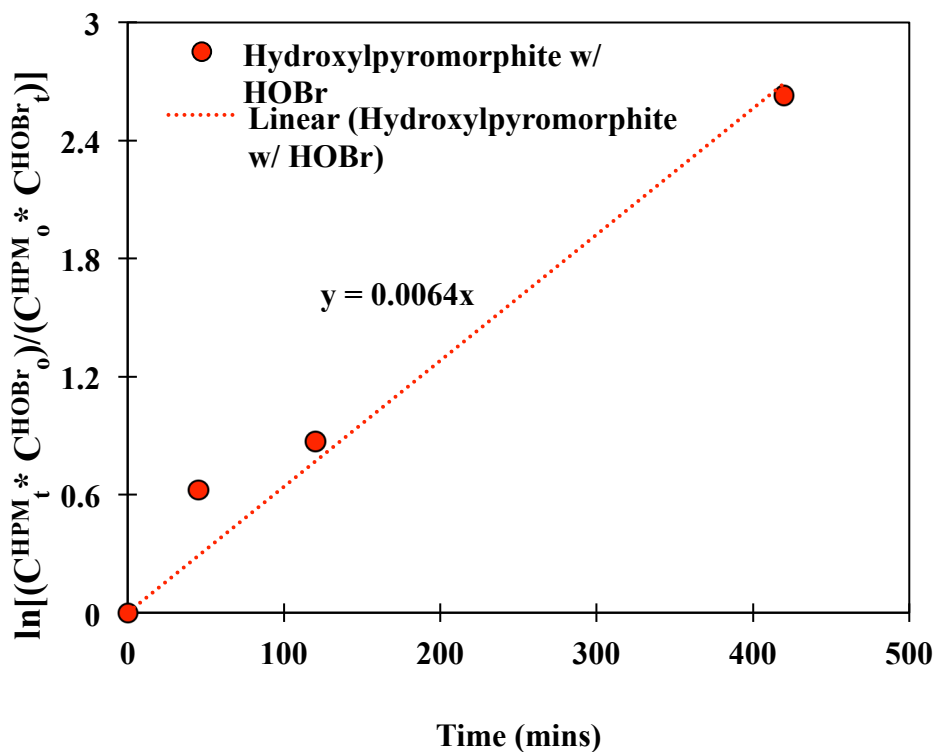


Figure S13 Estimation of reaction rate constant ($k^{\text{HOBr}}_{\text{Hydroxypyromorphite}}$) for hydroxypyromorphite (HPM) oxidation using HOBr, where C^{HPM}_t , C^{HPM}_0 and C^{HOBr}_t , C^{HOBr}_0 refer to concentrations of hydroxypyromorphite and HOBr at time time = t and time = 0, respectively.

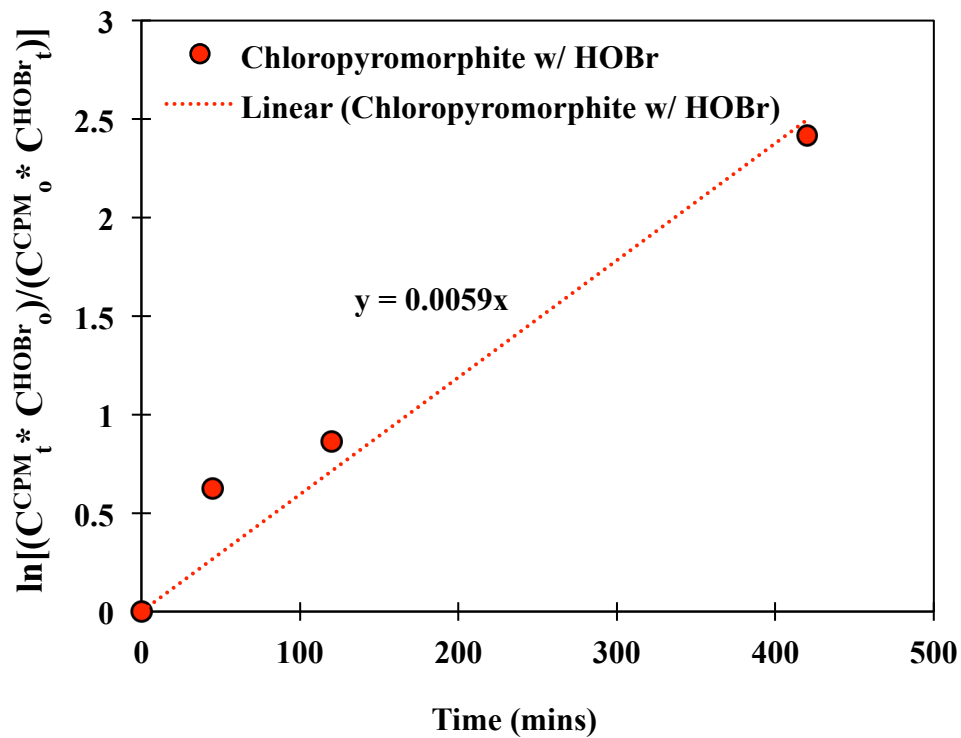


Figure S14 Estimation of reaction rate constant ($k^{\text{HOBr}}_{\text{Chloropyromorphite}}$) for chloropyromorphite (CPM) oxidation using HOBr, where C^{CPM}_t , C^{CPM}_0 and C^{HOBr}_t , C^{HOBr}_0 refer to concentrations of chloropyromorphite and HOBr at time time = t and time = 0, respectively.

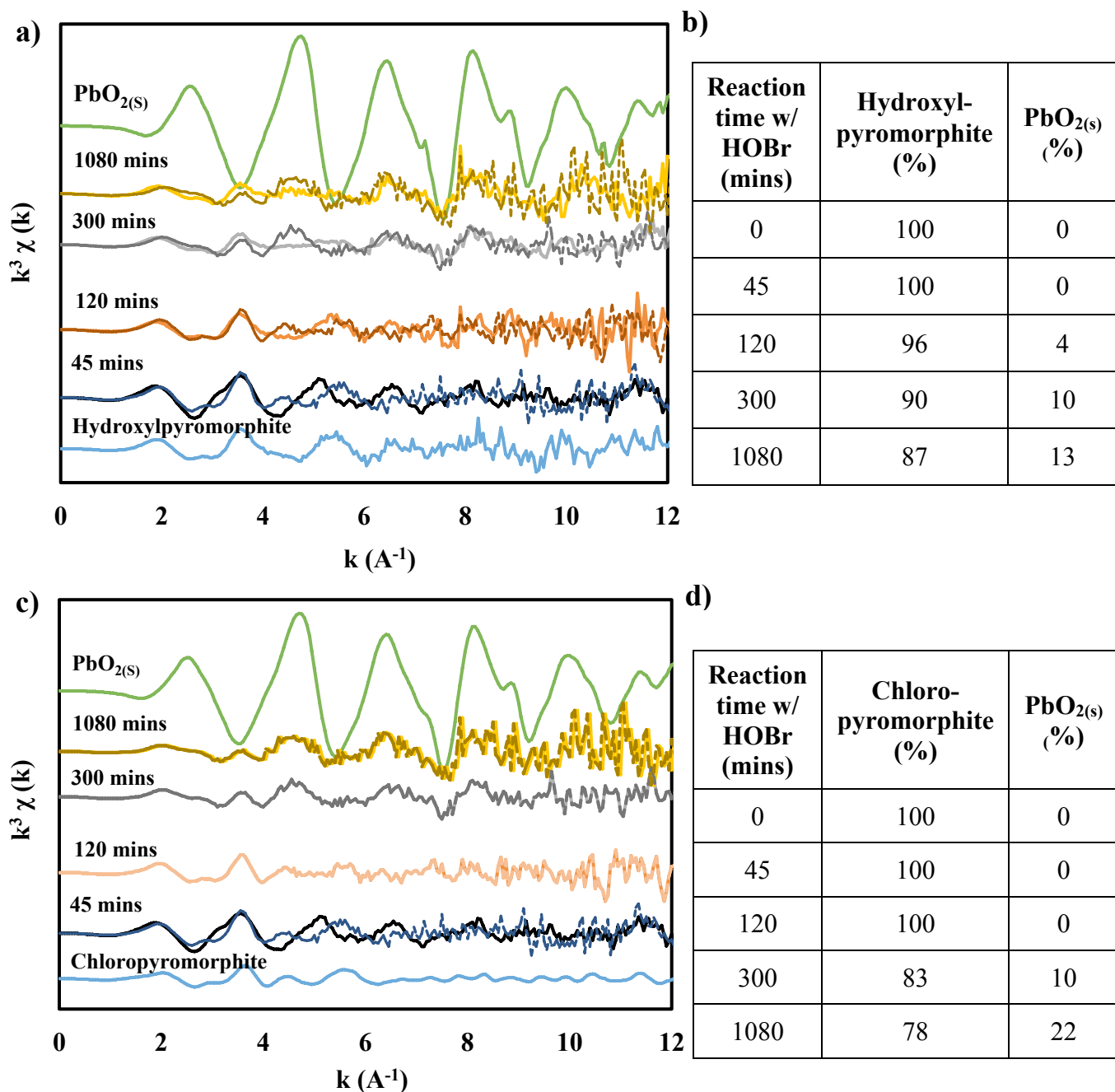


Figure S15 EXAFS spectra of lead phosphate oxidation by HOBr **a)** Hydroxylpyromorphite **c)** Chloropyromorphite. Percentage distribution of Pb(II) and Pb(IV) minerals in the solids during lead phosphate oxidation by HOBr. Linear combination fitting (represented by dashed lines) of the EXAFS spectra, **b)** Hydroxylpyromorphite **d)** Chloropyromorphite.

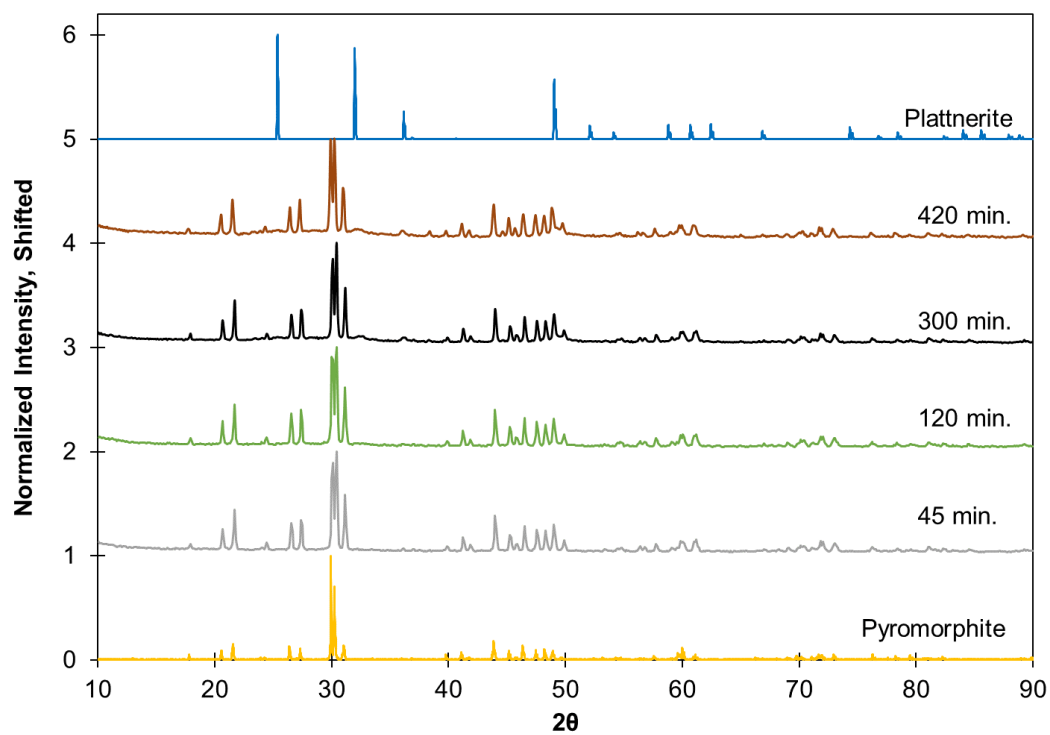


Figure S16 XRD spectra of lead solids during pyromorphite oxidation by free bromine. $\text{TOTCO}_3 = 10 \text{ mM}$, $[\text{HOBr}]_0 = 4.2 \text{ g/L as Cl}_2$, initial $\text{Cl}_2:\text{Pb(II)}=3:1$, $T=22^\circ\text{C}$, $\text{pH}=7$.

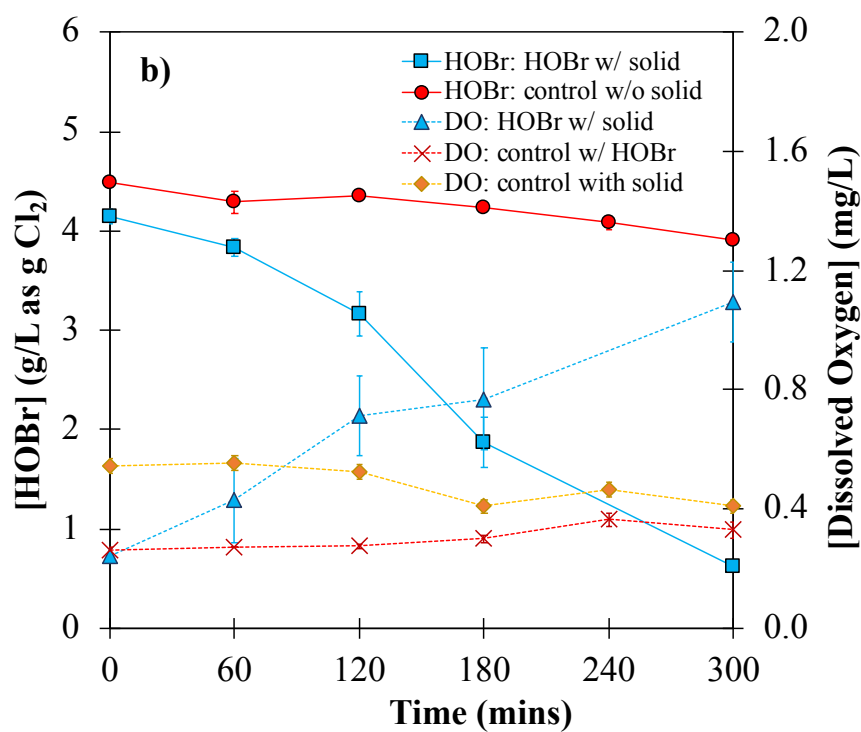
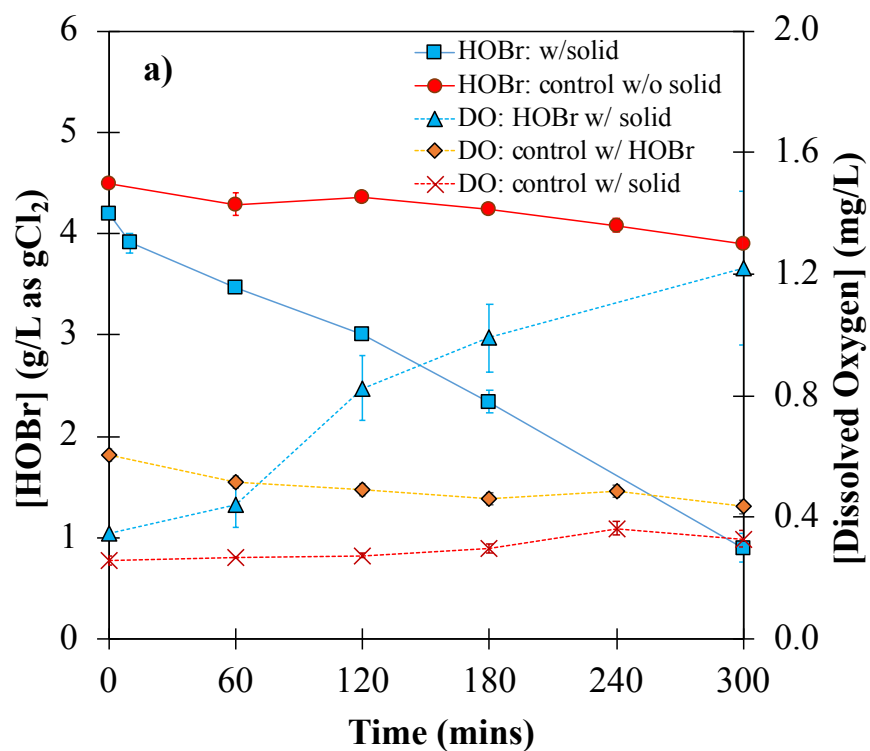


Figure S17 Dissolved oxygen (DO) measurement during lead phosphates oxidation by HOBr. $\text{TOTCO}_3 = 10 \text{ mM}$, $[\text{HOBr}]_0 = 4.2 \text{ g/L}$ (59.2 mM) as Cl_2 , initial $[\text{HOBr}]:[\text{Pb(II)}]=3:1$, $T=22^\circ\text{C}$, $\text{pH}=7$. **(a)** hydroxypyromorphite oxidation; **(b)** chloropyromorphite oxidation.